Article:
Nguyen, TTH orcid.org/0000-0002-6752-1455, Rosbottom, I orcid.org/0000-0001-6342-3973, Marziano, I orcid.org/0000-0002-3759-0070 et al. (2 more authors) (2017) Crystal Morphology and Interfacial Stability of RS -Ibuprofen in Relation to Its Molecular and Synthonic Structure. Crystal Growth & Design, 17 (6). pp. 3088-3099. ISSN 1528-7483

https://doi.org/10.1021/acs.cgd.6b01878

Crystal morphology and interfacial stability of RS-Ibuprofen in relation to its molecular and synthonic structure

Thai T. H. Nguyen[1+], Ian Rosbottom[1], Ivan Marziano[2], Robert B. Hammond[1], Kevin J. Roberts[1*]

1. *Centre for the Digital Design of Drug Products, School of Chemical and Process Engineering, Institute of Process, Research & Development, University of Leeds, Leeds, LS2 9JT, Leeds*

2. *Pfizer Worldwide Research and Development, Sandwich, CT13 9NJ, UK*

+ *New address: Department of Chemical & Process Engineering, James Weir Building, University of Strathclyde, Glasgow G1 1XQ*

Key words: intermolecular interactions, crystal habit faces, hydrogen-bonds, intrinsic (bulk) synthons, extrinsic (surface terminated) synthons, slice energy, attachment energy, solvent-mediated morphologies, crystallization process, growth mechanisms, α-factors, morphological instabilities, ibuprofen

Abstract

The key intermolecular (synthonic) interactions, crystal morphology and surface interfacial stability of the anti-inflammatory drug RS-ibuprofen are examined in relation to its bulk crystal and surface chemistry, and to rationalise its growth behaviour as a function of the crystallisation environment. The OH…O H-bonding dimers between adjacent carboxylic acid groups are calculated to be the strongest bulk (intrinsic) synthons, with other important synthons arising due to interactions between the less-polar phenyl ring and aliphatic chain.

Morphological prediction, using the attachment energy model predicts a prismatic facetted shape, in good agreement with the shape of the experimentally grown crystals from the vapour phase. Crystals grown from solution are found to have higher aspect ratios, with t hose prepared in polar protic solvents (EtOH) producing less needle-like crystals, than those prepared in less polar and aprotic solvents (toluene, acetonitrile and ethyl acetate). Though the anisotropy factors of the {011} and {002} forms are relatively similar (39.5% and 43.4% respectively), examination of the surface chemistry reveals that the most important extrinsic (surface-terminated) synthons on the capping {011} surface involve H-bonding interactions, whilst those on the side {002} surfaces mostly involve van der Waal's (vdW) interactions. This suggests that a polar, protic solvent is more likely to bind to the capping {011} surface and inhibit growth of the long axis of the needle, compared to apolar and/or aprotic solvents.

A previously unreported re-entrant face is found to appear in the external crystal morphology at higher supersaturations (in the range of $\sigma = 0.66$-0.79), not due to twinning, which is provisionally identified as being consistent with the {112} or {012} form. Analysis of the calculated surface entropy α-factors suggest that the capping {011} faces would be expected to be least smooth on the molecular level, with a higher degree of unsaturated extrinsic synthons, in comparison to the

{002} and {100} faces. This is consistent with growth mechanism data previously published[2], and with the observed re-entrant morphological instability at the capping surfaces.

List of Symbols:

E_{cr}: Lattice energy

E_{sl}^{hkl}: Slice energy per surface *hkl*

E_{att}^{hkl}: Attachment energy per surface *hkl*

Å: Angstroms

R_{hkl}: Relative growth rate per surface *hkl*

α_{hkl}: Alpha factor per surface *hkl*

ξ_{hkl}: Anisotropy factor *hkl*

ΔH_f: Enthalpy of fusion

R: Gas constant

T: Absolute temperature

X_{seq}: Mole fraction of solute

ΔH_{sub}: Sublimation enthalpy

BCF: Burton, Cabrera and Frank spiral growth mechanism

B & S: Birth and spread growth mechanism

RIG: Rough interfacial growth mechanism

Glossary:

vdW: van der Waals

H-bonding: Hydrogen bonding

Synthons: Pairwise intermolecular interactions

d-spacing: inter-atomic plane separation

Intrinsic Synthons: Fully saturated synthons found in the bulk of the crystal structure

Extrinsic Synthons: Unsaturated synthons due to surface termination of the crystal structure

Lattice Energy: Strength of the intermolecular interactions within the crystal structure per mol

Slice Energy: Energy of intermolecular interactions found within one d-spacing on the (*hkl*) crystallographic plane

Attachment Energy: Energy of intermolecular interactions formed when a slice one d-spacing thick is added to a surface defined by (*hkl*) plane

Anisotropy Factor: The degree of saturation of a molecule exposed at a cleaved crystal surface (*hkl*), in comparison to the same molecule fully saturated in the bulk structure

Jackson α-factor: Degree of roughening of a crystal surface (*hkl*) on the molecular level

1 Introduction

Anisotropically shaped crystalline materials can be problematic in downstream pharmaceutical product processing, in terms of powder flow, blending ability and formulation. The production of these non-ideal crystalline sizes and shapes can reflect the anisotropic nature of the structures of molecular crystals, leading to anisotropic face-specific growth rates. In order to produce particles of a desirable shape and size distribution from solution, it is important to understand and characterise the bulk crystal and surface chemistry and to relate how the crystal surfaces may interact with the surrounding solution during crystal growth.

Molecular and crystallographic modelling can be used to provide an insight into the relationship between structural aspects of molecular crystals and their resultant physical properties[3-9], which can minimise the need for extensive laboratory studies. Engineering crystallography techniques often utilise atomistic force fields to calculate the strength and direction of the molecule-molecule intermolecular interactions (synthons) within the crystal structure, and in-turn to use these calculations to predict the physical properties of the crystals[10-23]. Such interactions, when considered within the bulk crystallographic lattice, can be referred to as intrinsic synthons. In contrast, when such interactions are terminated and exposed at the growth surface, the associated molecules become partially unsaturated with respect to those in the bulk and can be referred to as extrinsic synthons[24]. The latter are important because they potentially have a significant impact on the physical and chemical properties of a crystalline particle, e.g. relative crystal growth rate of individual faces, particle shape and aspect ratio, reactivity, tendency to agglomerate etc. These concepts are encompassed within the emerging field of synthonic engineering[24, 25], which applies a retro-synthetic approach to the design of molecular crystals with pre-defined properties, based

on the making and breaking of synthons in the bulk of the material, and at the crystal solution interface.

For the case of the prediction and analysis of crystal morphologies, morphologically important surfaces can be selected based on the BFDH rule[26-28] and attachment energies can be calculated to predict the relative growth rates[29-33], the latter being based upon an assessment of the strength of the extrinsic synthons at these surfaces, to produce the expected morphology. The identification of the extrinsic synthons per surface (hk)l can also provide an insight into the nature of intermolecular interfacial interactions that govern the growth of the morphologically important surfaces[34].

The relative growth rate of a flat crystal surface growing in a stable manner via step terrace movement by e.g. a Burton, Cabrera and Frank mechanism (BCF)[35], or by a birth and spread mechanism (B&S)[36], can be assessed utilising the attachment energy model[30]. Though there have been a number of studies which have successfully predicted the morphology of crystals as a function of solvent environment for surfaces which grow by such mechanisms[12, 20, 37-41], a universal method for predicting the dependence of the crystal morphology as a function of solvent choice is yet to be fully established. It is though well-known that if a crystal surface grows with a roughened interface, then the crystal growth rate can be significantly increased[42-44]. However, such growth processes, through the loss of the intermolecular recognition inherent in surface step/terrace motion, can involve lower crystal perfection and, potentially lower crystal purity. With respect to identifying roughened interfaces, the calculation of α-factors, as introduced by Jackson in 1958[45], can be helpful in terms of assessing the surface interfacial roughness of a material. Jacksons initial work examined the transition from a singular to a rough growth interface for the case of a (001) face of a Kossel crystal growing from the melt phase[45, 46]. In this, the degree to which solid-solid

and fluid-fluid interactions are broken to make a solid-fluid interactions is assessed, with respect to the thermal process.

Further work by Bennema and co-workers considered the solution growth case and re-formulated the equation to account for wetting conditions in solution[6, 46-51], by correlating the making and breaking of solid-solid, solid-fluid and fluid-fluid interaction to the solubility of the material, and hence to its enthalpy of dissolution. In addition, to account for the inherent anisotropy between different crystal habit planes, differences between the fraction of solid-solid interactions per crystal slice (hkl), can also be taken into account, in comparison to the more simple Kossel crystal case. Therefore this formulation allows an assessment of the interfacial roughening per crystallographic surface. In this, a lower α-factor implies a rougher surface, and one tending towards a rough interfacial growth mechanism. Surfaces with increasing α-factors can be assessed to be smoother, consistent with a singular interfacial structure at the molecular level and one which can be predicted to grow by BCF or B&S growth mechanisms. For a particular crystal face growing from solution in different solvents and/or solute concentrations, the value of α can be expected to change depending on the degree of the solute-solvent interactions.

This paper draws upon the above perspective and applies a synthonic analytical approach to relating the bulk and surface crystal structural chemistry of RS-ibuprofen to its morphology and crystal growth from solution. In particular, it seeks to characterise the extrinsic (surface terminated) synthons at the crystal surfaces and assess how they might interact with the surrounding solution. The interfacial stability of the crystal habit surfaces is addressed through calculations of the surface entropy α-factors, and the resultant predicted growth mechanisms are confronted with previously published experimental data[2]. Overall, this study highlights the value

of achieving a molecular understanding of crystal and surface chemistry of RS-ibuprofen, in relation to the selection of solvents for its crystallisation.

2 Materials and methods

2.1 Materials

The ibuprofen molecule contains a carboxylic acid group at one end and an aliphatic chain at the other, split by a phenyl ring group (Figure 1(c)). Racemic (RS)-ibuprofen crystallises in a centrosymmetric tetramolecular monoclinic unit cell, shown in Figure 1(a) and (b).

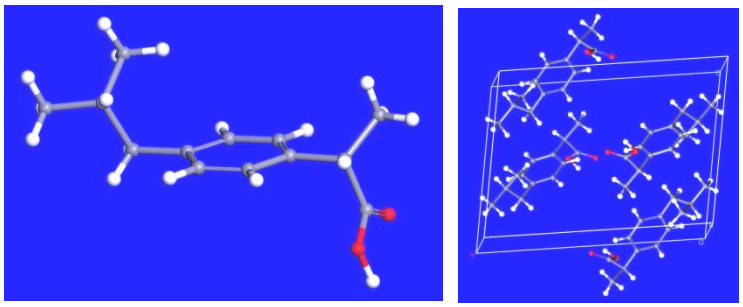

(a) (b)

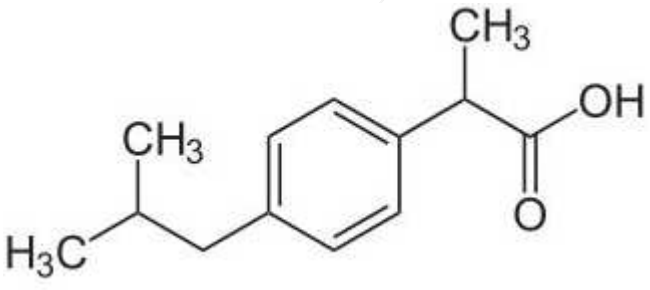

(c)

Figure 1: Molecular diagrams of Ibuprofen showing (a) the molecular structure and (b) packing within the crystallographic unit cell; (c) 2D molecular structure showing atom types

The unit cell is monoclinic with a $P2_1/c$ space group with the unit cell parameters: a = 14.68Å, b = 7.89Å, c = 10.73Å and β = 99.36°[52] (CCDC ref code: IBPRAC).

For the experimentally grown crystals, ibuprofen (≥98%) was purchased from Sigma Aldrich and Tokyo Chemical Industry UK Ltd. Ethanol (95%, the azeotropic composition of a binary ethanol and water mixture) and anhydrous toluene (99.8%) were purchased from Sigma Aldrich, ethyl acetate at 99.5% purity was purchased from Acros Organics and acetonitrile at 99.9% purity was purchased from LC-MS.

2.2 Intermolecular force calculations and morphology prediction

2.2.1 Intermolecular interactions and lattice energies

All calculations of the intermolecular interactions in this study used the Dreiding forcefield parameters[53] and partial atomic-charges that were calculated using the semi-empirical quantum mechanics program MOPAC[54], utilising the Austin Model 1(AM1) approach[55]. This approach has been extensively used in simulations of the behaviour of molecular crystals[10-13, 15, 31, 32, 56-61]. The crystal structure was optimised, via the minimisation of the calculated lattice energy, using the Forcite module within Materials Studio 5.5[62], keeping the unit cell and molecular structure rigid.

The intermolecular interactions were calculated and ranked by strength using HABIT98[63]. This calculation was then used to calculate the lattice energy (E_{cr}). The calculated lattice energy was compared to the experimental sublimation enthalpy (ΔH_{sub}) to ascertain whether the forcefield selected accurately estimated the intermolecular strengths between the molecules, since the lattice energy and sublimation enthalpy are related through Equation (1).

$$E_{cr} = \Delta H_{sub} - 2RT \qquad (1)$$

Where R is the gas constant and T is the temperature at which the sublimation enthalpy was measured.

The lattice energy convergence was checked increasing the diameter of the radius of calculation by 1Å steps, up to 30Å. The percentage of lattice energy added with each 1Å step was also calculated.

2.2.2 Morphological prediction and determination of extrinsic synthons

The morphologically important surfaces were calculated using the BFDH method[26-28], in MORANG[64]. For each of the identified morphologically important surfaces, the lattice energy was then was partitioned with respect to their contribution to the growth process through the calculation of slice (E_{sl}) and attachment (E_{att}) energies for each crystal habit surface (Equation (2)).

$$E_{cr} = E_{att}^{hkl} + E_{sl}^{hkl} \quad (2)$$

Synthons were characterised in terms of whether they were intrinsic (bulk), i.e. contributing to the slice energy, or if they were extrinsic (surface terminating) and contributing to the attachment energy, for each of the selected crystal forms. With the intermolecular interactions calculated, the most stable slice was identified by shifting the slice boundary by 0.1 d-spacing until the smallest absolute value of the attachment energy was found, this was assumed to be the most stable termination of the surface. The attachment energies were assumed to be directly proportional to the relative face specific growth rates[5] (Equation (3)).

$$R_{hkl} \propto E_{att}^{hkl} \quad (3)$$

The attachment energies were scaled as centre to face distances and a Wulff plot was constructed using SHAPE[65].

2.2.3 Surface entropy α-factors

The α-factors were calculated using the following expression[43, 47-51, 66]

$$\alpha = \xi_{hkl}\left(\frac{\Delta H_f}{RT} - lnX_{seq}\right) \quad (4)$$

where ΔH_f is the heat of fusion; X_{seq} is the mole fraction of the solute as calculated for the supersaturation typically considered for crystal growth for a given solvent and temperature, R is the ideal gas constant and T is the absolute temperature. The anisotropy factor, ($\xi_{hkl} = {E_{sl}^{hkl}}/{E_{cr}}$), reflects the degree of saturation of a molecule when it is surface terminated and a fraction of the intermolecular interactions have been broken. Hence, it is a measure of the degree of intermolecular interactions saturated for a molecule exposed at a particular crystal surface (*hkl*), when compared to a molecule fully saturated in the bulk of the structure.

The numerical values of α can be correlated to a given surface's interfacial roughness on the molecular level[49], shown in Table 1.

Table 1: Predicted growth mechanism according to the value of α[47, 48, 50, 51]

α-factor range	Predicted growth mechanism
α < 2	The interface is rough hence all growth units can be incorporated onto the growing surface (continuous growth).
2 < α < 5	The interface is smoother and the most probable mode of growth is B&S
α > 5	The surface becomes very smooth and growth generally proceeds by screw dislocation (BCF).

2.3 Crystal growth and characterisation

2.3.1 Crystal growth and optical microscopy

The ibuprofen crystals presented in this paper were grown at an 0.5ml scale, as detailed in a previous paper[2]. The crystallisation setup employed for this comprises an inverted optical polarizing microscope (Olympus Optical IMT-2 or Leica/ Leitz DM IL 090-131-002) integrated with a CCD Lumenera Infinity 3.3 megapixel camera and a PC with Infinity II Image Capture and Image Analyze Software, to capture pictures during crystal growth. The crystallisation vessel comprised of a UV cuvette cell 0.5ml (54 x 10 x 1 mm) submerged in a shallow tank of water whose temperature was controlled by a Haake F3 recirculation bath. RS-ibuprofen solutions were prepared by dissolving solute in ethanol 95% (1.4g/ml), ethyl acetate (1g/ml), acetonitrile (0.4g/ml) and toluene (1g/ml). A pipette was used to transfer the prepared solution into the cuvette cell, which was sealed and fixed to the bottom of the water tank. The ibuprofen/solvent solutions were heated to 50°C to completely dissolve all ibuprofen crystals, then the solutions were cooled down to a constant temperature such as 20, 23, 25 and 27°C to maintain a specific supersaturation until crystals were found to appear.

2.3.2 Determination of interplanar angles

The interplanar angles between the surfaces proposed to be present on the external crystal morphology were determined using the MORANG program[64], which uses the unit cell information to calculate the angle between the planes defined by *hkl*. The experimental interfacial angles were measured as shown in Figure 2, derived from the optical microscopy images taken from the experiments described in Section 2.3.1 (Figure 2).

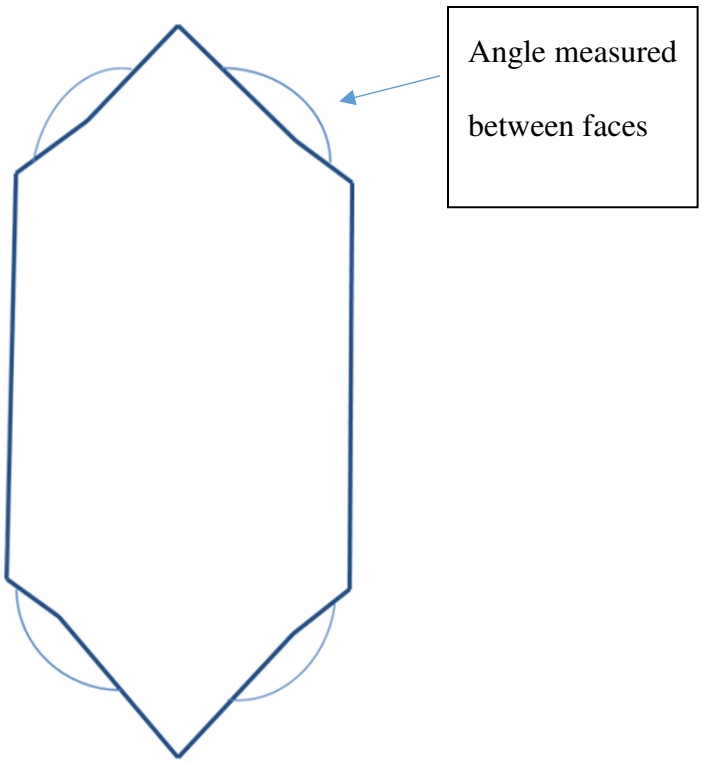

Figure 2: Example of how the interplanar angles are measured from an optical microscopy image of a crystal

3 Results and discussion

3.1 3D crystal chemistry

The intermolecular packing and crystal chemistry of ibuprofen is shown in Figure 3.

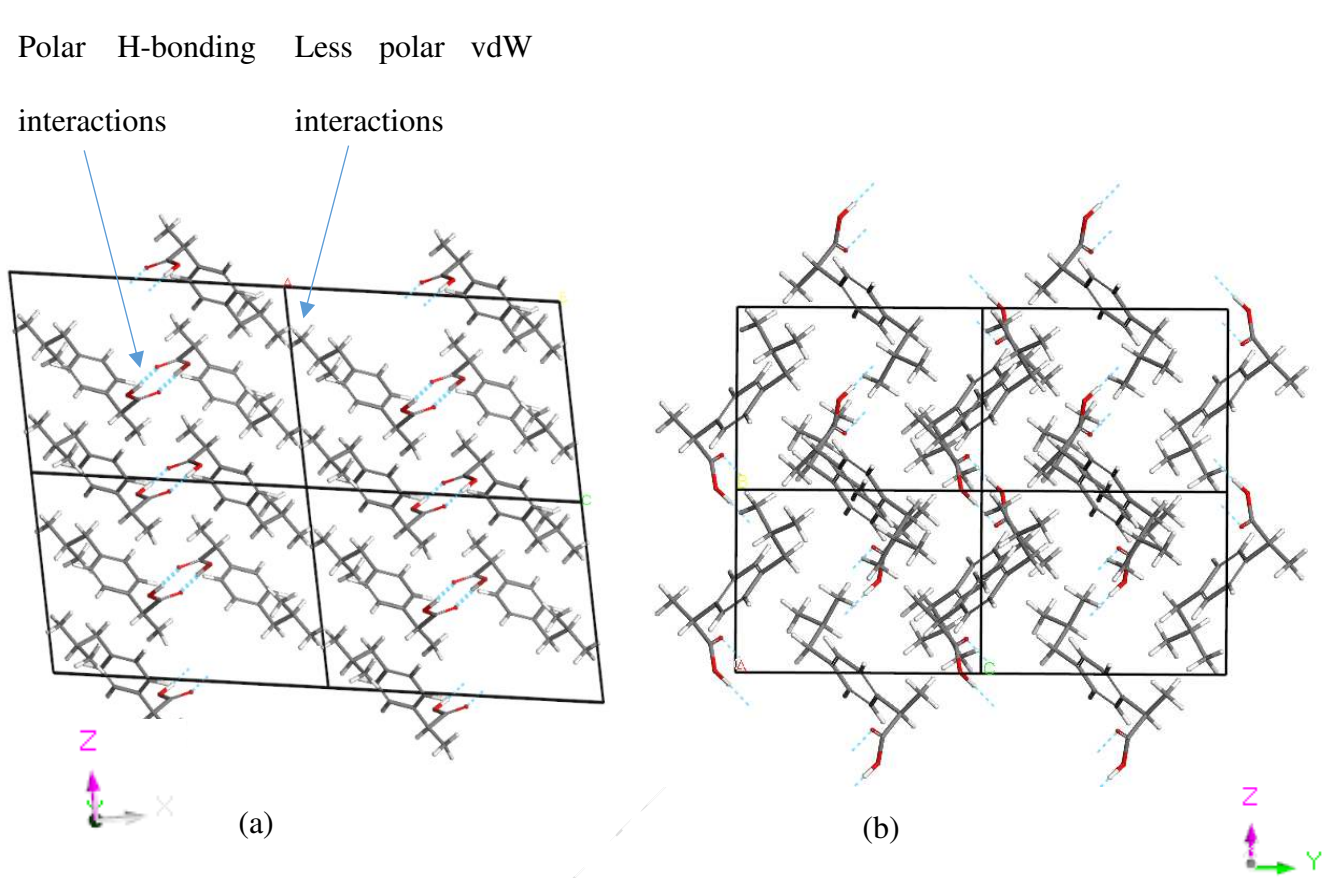

Figure 3: Molecular packing of ibuprofen (a) looking down the <010> direction; (b) looking down the <100> direction

Figure 3(a) shows that polar and apolar components of the ibuprofen molecule interact alternately, approximately along the x-direction, allowing the formation of the OH…O H-bonding carboxlyic acid dimers. The presence of the aliphatic chain probabaly inhibits the close packing of the aromatic ring moeties, that has been observed molecular crystal structures accomodating less bulky molecules[34, 67, 68].

Figure 4 shows the strongest calculated bulk synthons, along with Table 2 showing their energetic breakdowns.

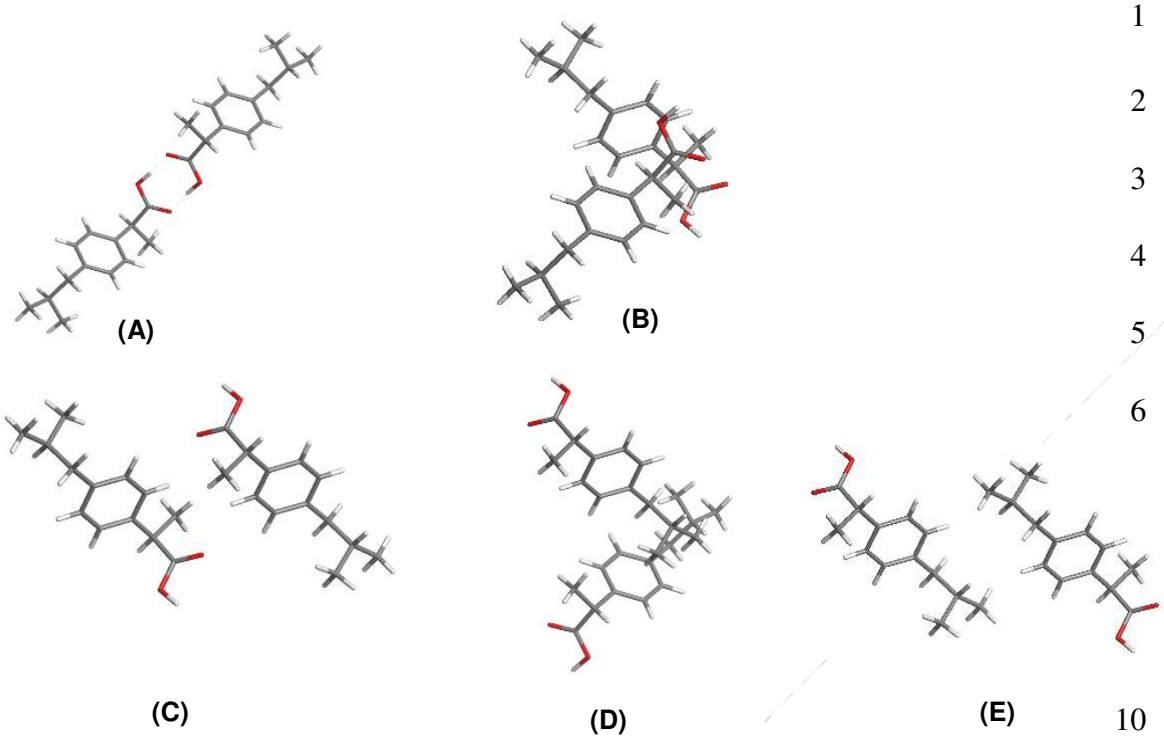

Figure 4: Pairwise molecular orientation of the 5 strongest synthons (A), (B), (C), (D) and (E) calculated from the bulk crystal structure of ibuprofen and shown in Table 2

Table 2: The top five synthons in the crystal lattice of ibuprofen based on intermolecular strength, along with their contributions to the lattice energy; the split of the synthon strength into H-bond+vdW and coulombic; the contribution of the functions groups to each synthons energy. All energies are quoted in kcal

Synthon	Multiplicity	Interaction Energy (kcal/mol)	% Contribution to the Lattice Energy	Type of interaction		Nature of functional group involved		
				vdW + H-Bond %	Coul %	Aliphatic %	Phenyl %	COOH %
A	1	-5.2	18.1	44.0	56.1	4.7	0.5	94.8
B	2	-2.8	19.5	89.4	10.6	46.0	38.7	15.1
C	2	-2.4	16.8	99.6	0.4	63.1	34.7	2.1
D	1	-2.2	7.7	65.9	34.1	38.4	42.44	19.2
E	1	-1.5	5.1	97.3	2.7	46.7	48.5	4.8

The strongest intrinsic synthon was calculated to be the OH…O H-bonding interactions between adjacent carboxylic acid groups (A). The OH…O H-bonds resulted in the total intermolecular strength of this synthon being calculated as over 2 kcal stronger than the next strongest interaction. Over 94% of this synthon energy was found to be centred on the COOH groups of the molecules involved, indicating that this interaction would be very directional in nature. In contrast, the COOH group plays a relatively minor role within the other major synthons, since there is no other polar proton available to interact with the remaining lone pair on the carbonyl oxygen.

3.2 Lattice energy

The lattice energy convergence as a function of limiting radius of the calculation is shown in Figure 5(a), along with the addition of energy as more molecules are added to the crystal structure as the limiting radius is increased, with respect to the origin molecule (b). This is shown as a tower graph with each tower representing the percentage of the energy added at the step, i.e. the tower at 7Å is the amount of energy added with the increase between 6Å and 7Å of the radius of the sphere.

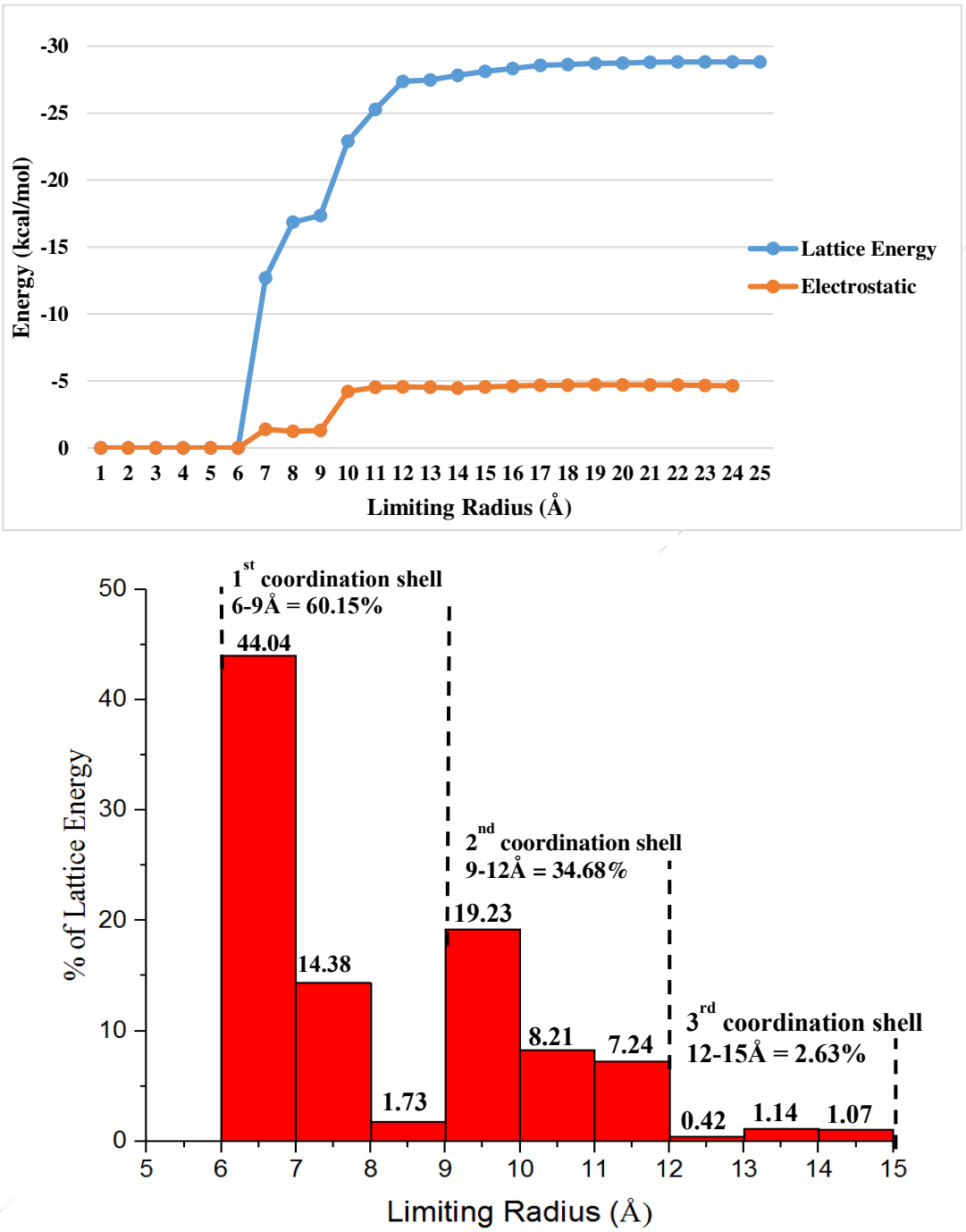

Figure 5: (a) Lattice energy as a function of increasing limiting radius of the sphere of calculation; (b) the % of the lattice energy added with the increase in radius of the sphere

The fully converged calculated lattice energy was -28.86kcal/mol (Figure 5(a)), which was in good agreement with the experimental lattice energy calculated from the heat of sublimation for ibuprofen of 30.10 kcal/mol[1]. This suggests that the Dreiding potential provides an acceptable reproduction of the strength and nature of the synthons within the crystal structure. It was also observed that the coulombic interactions contributed a relatively small amount to the lattice energy, perhaps reflecting that the majority of the molecule is apolar in nature. This is consistent with to the fact that only the H-bonding COOH group within the ibuprofen molecule which contains significantly electronegative atoms to contribute to the polar nature of the molecule.

Figure 5(b) indicates that there are three major coordination shells of energy between 6Å and 15Å, where the first shell between 6Å and 9Å was found to contain over 60% of the lattice energy. The second and third shells were calculated to contain 34.68% and 2.63% respectively, highlighting the rapid decrease in the importance of the synthonic interactions with distance in the ibuprofen structure. This highlights the importance of the nearest neighbours for stabilising the crystal lattice energy of molecular crystals, such as ibuprofen.

3.3 Crystal morphology

3.3.1 Attachment energy morphological prediction

The calculated surface attachment energies for the morphologically important forms are given in Table 3, with the predicted morphology based on these values in Figure 6.

Table 3: For the morphologically important surfaces of ibuprofen: interplanar spacing (in Å); slice and attachment energies (in kcal/mol); anisotropy factors calculated from Equation (4) and multiplied by 100 to give %; α-factors between 15°C-35°C for ethanol, ethyl acetate, acetonitrile & toluene

		Attachment energy Information			Face specific α-factors between 15°C-35°C			
Face	**d_{hkl} (Å)**	**E_{sl}^{hkl}(kcal/ mol)**	**E_{att}^{hkl} (kcal/mol)**	**ξ_{hkl}**	**Ethanol**	**Ethyl acetate**	**Acetonitrile**	**Toluene**
{100}	14.4	-24.2	-4.6	84.0	9.4 – 10.6	9.3-10.4	10.3 – 12.1	9.3-10.5
{110}	7.0	-12.8	-16.0	44.4	5.2-5.6	4.9-5.5	5.5 - 6.4	4.9-5.6
{011}	6.9	-11.4	-17.5	39.5	4.6-5.0	4.4-4.9	4.8 – 5.7	4.4-4.9
{111}	6.0	-12.0	-16.9	41.5	4.8-5.2	4.6-5.2	5.1-6.0	4.6-5.2
{002}	4.3	-12.5	-16.3	43.4	5.0-5.5	4.8-5.4	5.3-6.2	4.8-5.4
{012}	5.3	-7.6	-21.2	26.4	3.1-3.3	2.9-3.3	3.2-3.8	2.9-3.3
{112}	4.1	-8.8	-20.0	30.6	3.5-3.9	3.4-3.8	3.8-4.4	3.4-3.8

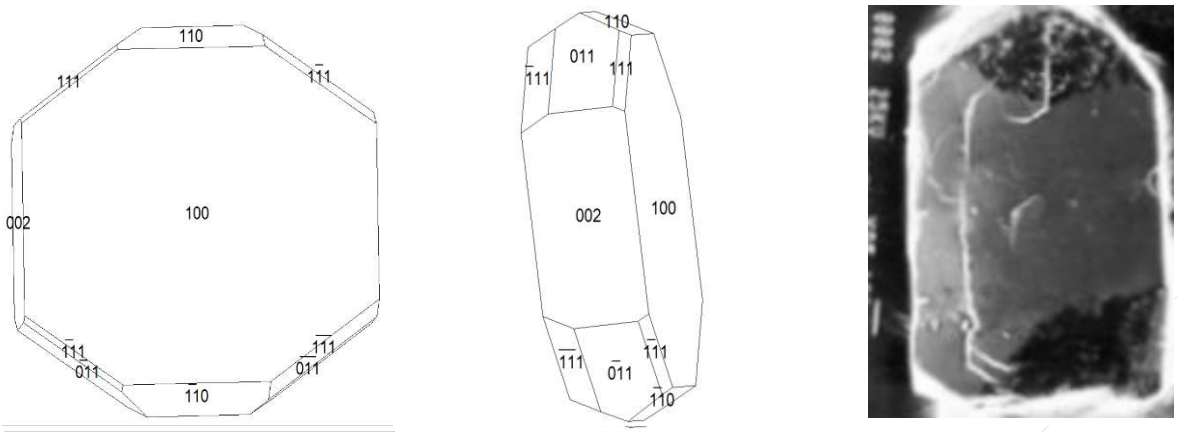

(a) (b) (c)

Figure 6: (a) attachment energy morphology prediction of ibuprofen looking down the (100) face; (b) looking down approximately the (002) face; (c) vapour grown crystal morphology of ibuprofen[1]

The morphological prediction with the dominant {100}, {002} and {011} forms was in reasonable agreement with previous studies[9, 69], and with the experimentally observed morphology of crystals grown from the vapour phase[1, 70, 71]. The {100} form had lowest attachment energy and highest percentage of satisfied synthons at the surface (column 5, Table 3), and therefore was predicted to be the slowest growing face of ibuprofen, which was in good agreement with the plate-like morphology with a dominant {100} form[2, 9].

3.3.2 Crystal morphologies from solution

The experimental morphologies produced from different solvents are shown in Figure 7.

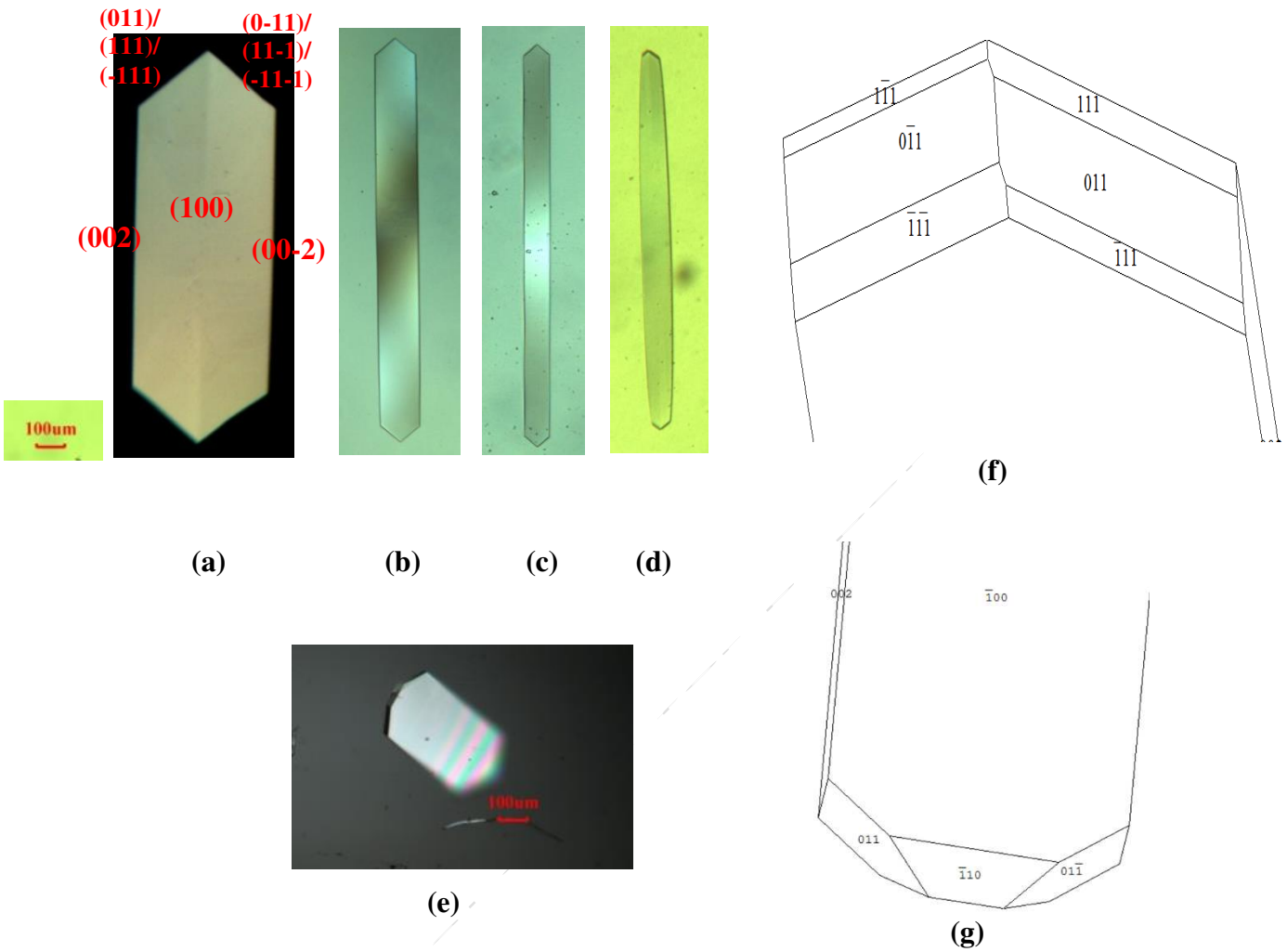

Figure 7 (i) Morphology of ibuprofen re-crystallised in (a) ethanol[2]; (b) ethyl acetate[2]; (c) acetonitrile[2]; (d) toluene[2]; (e) thin crystal morphology of ibuprofen re-crystallised in ethanol solutions[2]; (f) possible faces predicted to be the capping faces of ibuprofen by attachment energy theory; (g) morphological sketch of the capping faces shown in the experimentally produced crystal in (e)

Figure 7 reveals that all the solvents tested produced crystal shapes that were similar to the morphologies calculated from the attachment energy model, except that the aspect ratio was found to vary between the solvents. The length along the b-axis of the solution grown crystals were found to be generally higher than the attachment energy morphology prediction, and the aspect ratio

observed for the crystal grown from the vapour phase (Figure 6(c)). The crystals produced from ethanol were observed to have the lowest aspect ratio, whilst the crystals produced from toluene and acetonitrile had the largest aspect ratios. This suggests that the growth of the {011} form was least hindered in aprotic solvents, resulting in the needle shaped crystals shown in Figure 7((b), (c) and (d)). In addition, Figure 7(e) shows that crystals produced from ethanol are very thin, indicating that the {100} face does indeed grow very slowly. This figure also suggests that the {110} form can sometimes appear between the {011} surfaces, consistent with the attachment energy simulation.

3.3.3 Morphological stability at the capping surfaces

Images of the crystals grown in the different solvents and at varying supersaturation are shown in Figure 8, to compare the morphological features of the crystals as a function of solvent and supersaturation.

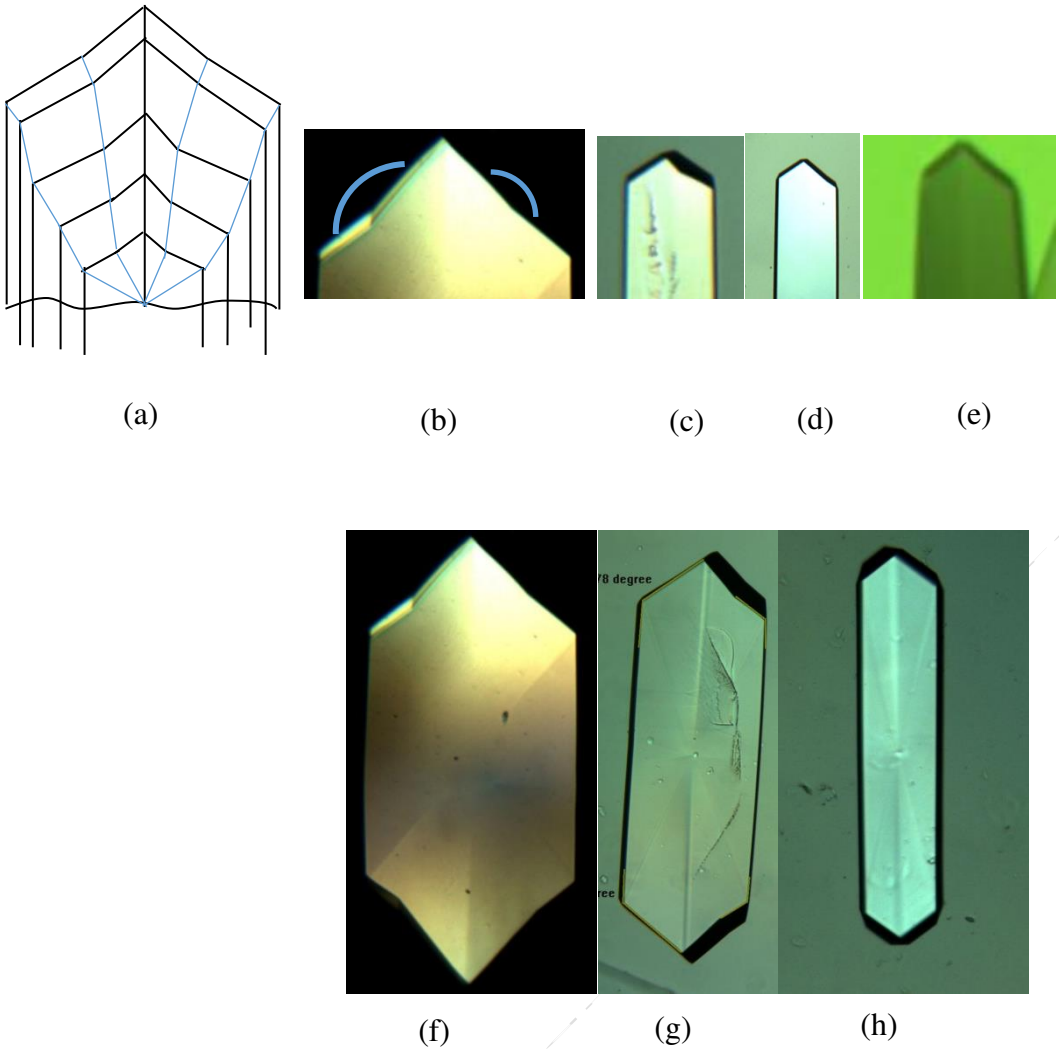

Figure 8: (a) Schematic diagram illustrating the growth history of the capping faces around the {011} surfaces highlighting the various sector zones involved and their growth sector boundaries together with a putative model for the nucleation of the re-entrant face; ibuprofen crystals grown from (b) ethanol, (c) acetonitrile, (d) ethyl acetate, and (e) toluene, with high index re-entrant faces showing that the re-entrant can occur in all solvents examined. The crystals shown in (f), (g) and (h) are crystallised from ethanol at σ = 0.97, σ = 0.79 and σ = 0.66 respectively, indicating that the re-entrant is more likely to occur at enhanced supersaturation

Figure 8 displays that an additional and re-entrant habit face was observed in all solvents, but only at high levels of supersaturation (σ = 0.66-0.79). The observation was found to be reproducible and present in the crystals grown from the solvents studied here. Figure 8(a) schematically

demonstrates a putative model for how the re-entrant facet develops as a function of time from the nucleation point at the capping faces of the crystal.

The critical supersaturations (σ_{crit}) associated with the occurrence of the re-entrant face are shown in Table 4.

Table 4: The critical supersaturation σ_{crit} for the appearance of the re-entrant faces

	Ethanol	Ethyl acetate	Acetonitrile	Toluene
Critical supersaturation σ	0.66	0.69	> 0.79	> 0.79

For acetonitrile and toluene, these re-entrant faces are present at a slightly higher value of σ_{crit} > 0.79. This may reflect the more needle-like crystals that are produced in these solvents, particularly in toluene. However, it was found to be challenging to monitor at what point the re-entrant was observed between the (011) and (0-11) surfaces, due to the small surface area of this face.

The re-entrant crystals shown in Figure 8 showed no obvious evidence of twinning, as confirmed using polarised optical microscopy[72], shown in Figure 9(ii).

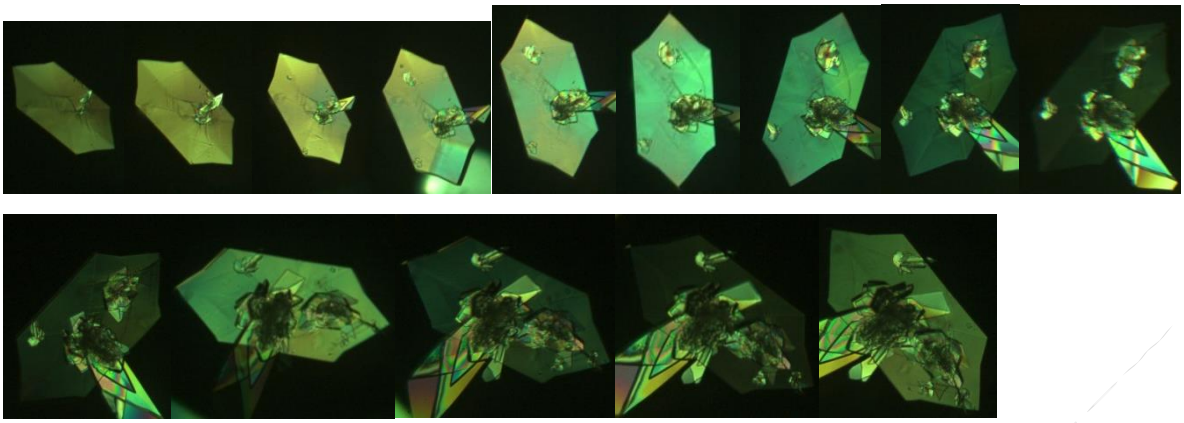

Figure 9: A series of polarized-light micrographs of ibuprofen crystals with the angle between cross-polarisers being increased by 30° between adjacent images. The images show that the crystals became homogeneously darker or brighter, proving that the re-entrant (concave) edges are not consistent with twinning.

Examination of the crystal morphology by crystallographic zone analysis[73], drawing upon the likely low index morphological habit planes identified from the BFDH analysis[32], revealed that characterisation of the interplanar angle over a range of samples prepared for all solvents used confirmed a consistency of interplanar angle of approx. 166° ± 2.7 between the re-entrant face and the (011) face, consistent with it being the same face re-entering in each sample and was not solvent dependent.

These re-entrant edges occur between the symmetrically equivalent faces (011) and (0-11). Analysis of the interplanar angles for this material, with the aid of morphological simulation, was consistent with the re-entrant planes being within the [0-21] zone comprising the (012) or (112) and (100) faces. The attachment energies of the (012) and (112) surfaces were calculated to be very close.

The occurrence of re-entrant morphological features, in the absence of twinning, is comparatively quite rare. Despite this, the natural development of a re-entrant facet is not forbidden from morphological theory[74, 75]. The fact that these facets appear at higher supersaturations and at the

end-capping habit faces, suggests that the mass-transfer effects are playing the dominant role in initiating the formation of the new faces. For needle shaped crystals, the solid angle sub-tended by the capping faces with respect to the solution, is much higher than that of the slower growing faces.

The end faces have a much higher degree of unsaturation in terms of their intermolecular interactions ($\boldsymbol{\xi_{hkl}}$, Table 3) and this might suggest that the growth kinetics for these faces would be mass-transfer limited, compared to the slow growing faces where the interfacial kinetics associated with solute integration into surface step/kink sites might be much more rate limiting. This high flux of molecules at the capping surface, driven by the high supersaturation, probably induces the surface nucleation, and hence the appearance of the observed re-entrant morphological feature.

3.4 Surface chemistry of the morphologically important surfaces

In a previous study, the surface chemistry of the major faces of ibuprofen was qualitatively described[2]. In this study the synthons that are predicted to contribute to the attachment energy, and hence growth, of a given surface have been identified and displayed in Table 5.

Table 5: Synthon analysis for the {011}, {001} and {100} forms with for a growth unit based on a monomer. For each of the four morphologically important forms it is identified whether the top 5 synthons contribute to the slice energy or attachment energy (marked red)

		Slice Energy (E_{SL}) or Attachment Energy (E_{ATT})			
Synthon type	**Interaction Energy (kcal/mol)**	**{011}**	**{002}**	**{100}**	**{110}**
A	-5.21	**E_{ATT}**	E_{SL}	E_{SL}	**E_{ATT}**
B	-2.82	**E_{ATT}**	**E_{ATT}**	E_{SL}	E_{SL}
C	-2.42	**E_{ATT}**	**E_{ATT}**	E_{SL}	**E_{ATT}**
D	-2.23	E_{SL}	**E_{ATT}**	E_{SL}	**E_{ATT}**
E	-1.49	E_{SL}	**E_{ATT}**	**E_{ATT}**	**E_{ATT}**

For the faces listed in Table 5, the extrinsic synthons identified to contribute to the attachment energies of these faces were labelled on molecular models of the surface, manifesting in perfect termination of the crystal structure. The molecular surface chemistry of the faces listed in Table 5 is shown in Figure 10.

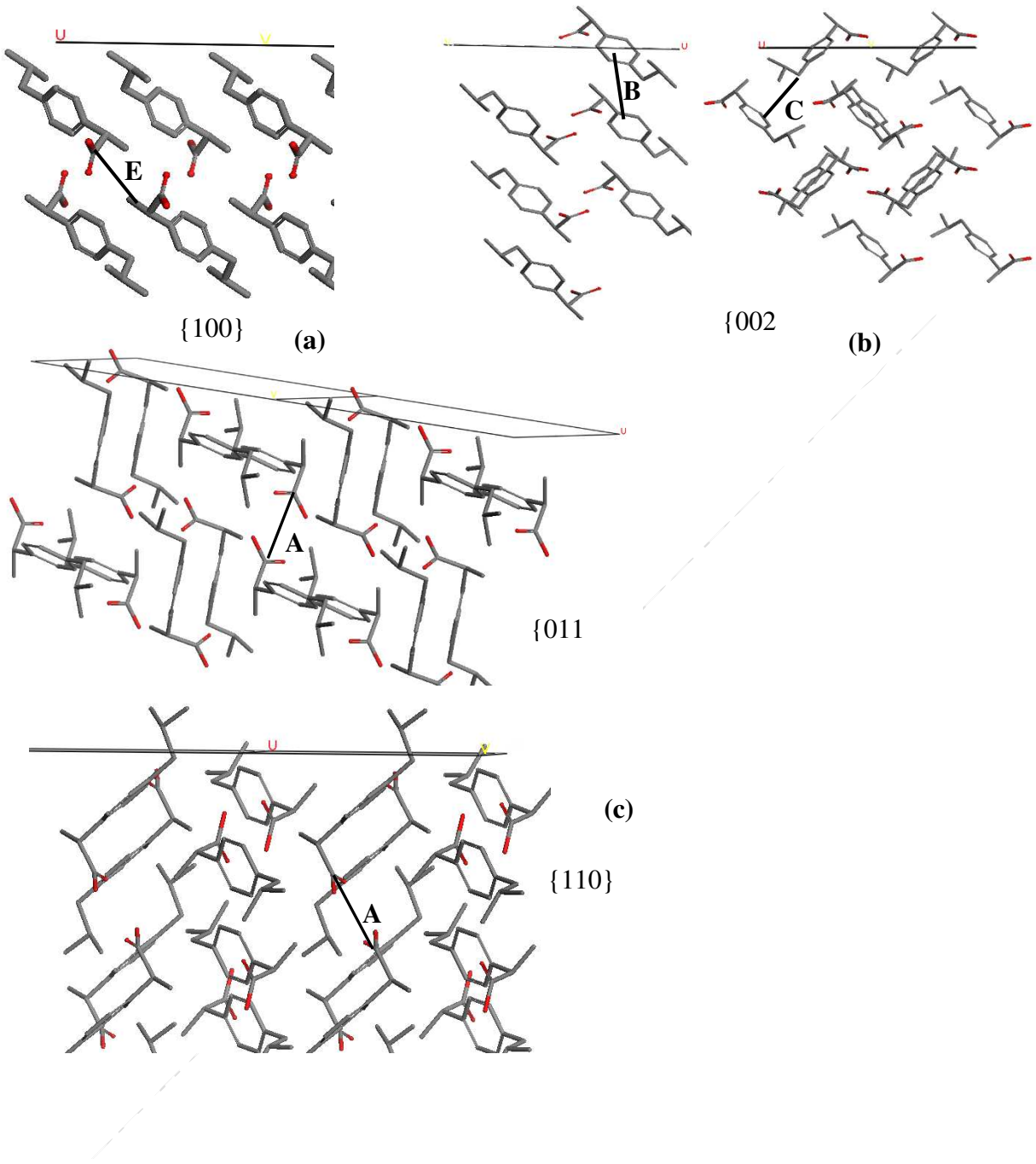

Figure 10: (a) Molecular orientation at the {100} face with synthon E marked on as contributing to the attachment energy of this surface; (b) molecular orientation of the {002} surface with synthons B and C marked on as contributing to the attachment energy of this surface; (c) molecular orientation of the {011} surface (above) and {110} surface (below) with synthon A marked on as contributing to the attachment energy of this surface

Figure 10(a) reveals that the strongest interaction contributing to the attachment energy at the {100} surface was found to be synthon E, which is the vdW interaction between adjacent aliphatic chains and the COOH groups. The weak nature of the interactions at this surface is consistent with the low attachment energy and slow growth, ultimately explaining the morphological dominance of this face and the resulting thin crystals obtained (Figure 7(e)).

Figure 10(b) reveals that synthons (B) and (C) contribute to the attachment energy of the side {002} form. These synthons were identified to be dominated by vdW interactions, and both are stronger than synthon (E), resulting in faster growth for the {0 0 2} form, and lower morphological importance compared to the {100} form.

Figure 10(c) reveals that synthon (A) contributes to the attachment energies of the capping {011} and {110} surfaces, and therefore would be expected to have a significant influence on the growth along the b-axis. However, Table 5 reveals that synthon (B), which was identified to be dominated by vdW interactions, has a significant impact on the growth of both the {011} and {110} forms. Hence, growth was predicted to be driven by both H-bonding and vdW interactions along the long axis of the needle, though only the growth of the capping surfaces were predicted to be strongly influenced by the OH…O H-bonding interactions.

It is likely that the variation in the strength and nature of the synthons which influence the growth of the different habit surfaces, is at the root of the dependence of the ibuprofen morphology on the nature of the growth solvent. The lower aspect ratio and more defined crystal morphology of crystals produced from ethanol is likely due to the ethanol molecules being able to act as both a H-bonding donors and acceptors, thus inhibiting the formation of the H-bonds (synthon (A)), and in turn decreasing growth rates along the long axis of the needle. The crystals with highest aspect ratios were produced from toluene (Figure 7d) and previously it was shown that the relative growth

rate of the {002} forms was lowest in toluene solutions[2]. The synthons at the {002} surface are predominantly vdW interactions between the phenyl ring and aliphatic chains of ibuprofen. Hence it could be expected that toluene molecules could inhibit the growth of the {002} face, whilst not hindering the growth of the {011} face, whereby the growth is more dominated by H-bonding interactions.

3.5 Correlation between the calculated α factor and the growth mechanism

The surface interfacial roughness, as well as the molecular surface chemistry, can also strongly influence the growth mechanism and growth rate of a crystal surface[47, 49, 51, 66]. Therefore the growth mechanisms and degree of interfacial roughness, calculated from the α-factors in Table 3 were compared for the morphological important surfaces, and to the previously published experimental data for the {011} and {002} surfaces, in Table 6.

Table 6: Comparison of calculated growth rate mechanisms from the α-factors in Table 3 to the previously published experimentally measured growth mechanisms

	{011}		{002}	
Solvent	**Predicted Growth Mechanism from α-factors**	**Experimentally Measured Growth Mechanism[2]**	**Predicted Growth Mechanism from α-factors**	**Experimentally Measured Growth Mechanism[2]**
Acetonitrile	BCF or B&S	B&S	BCF	B&S
Ethanol	B&S	BCF/B&S	BCF or B&S	BCF/B&S
Ethyl Acetate	B&S	B&S	BCF or B&S	B&S
Toluene	B&S	B&S	BCF or B&S	B&S

The α-factors calculated for the solvents examined in this study were found to match well to the experimental growth mechanisms that have been previously identified for the {011} and {002} surfaces[2]. The calculated α-factors indicated that the surfaces that were predicted to be present at the capping end faces of the crystal from Figure 6, such as the {011}, {110} and {111} surfaces (Table 3), were predicted to be more rough than the other surfaces on the final crystal morphology. The ibuprofen crystals are observed to needle along the b-axis in acetonitrile, ethyl acetate and toluene (Figure 7), whereby the increased roughening of these capping habit faces could increase the probability of overgrowth and needling along the direction of the growth normal of these

surfaces. In addition, the {012} and {112} faces, which were identified as the likely re-entrant facets, were also calculated to be even rougher than the other capping facets, correlating well to the supposition that the interfacial roughening at these surfaces results in the morphological instability and re-entrant facets.

4 Conclusions

The detailed surface chemistry of ibuprofen has been characterised and linked to the crystal morphology from four solvents, along with a prediction of the crystal growth rate mechanisms and interfacial stability using α-factor calculations. The shorter aspect ratio morphology observed in ethanol, compared with the less polar and aprotic solvents, was correlated to supposition that the polar and protic nature of EtOH makes it more likely to be able to disrupt the OH…O interactions in synthon (A) that were identified to influence the growth along the long axis of the needle, hence reducing the growth rate along the long axis of the morphology.

The α-factors suggest that the capping {011} surfaces are rougher on the molecular scale, when compared to the other morphologically important surfaces, hence correlating to the increased growth rate at these surfaces that result in the needle-like morphologies. The good agreement between the predicted and experimentally derived crystal growth mechanisms suggested these calculations are relatively robust. The observation of a previously un-reported re-entrant face between the (011) and (01-1) surfaces could be indicative of the increased interfacial roughening at the capping faces, resulting in this morphological instability.

This combination of molecular modelling of the synthons, combined with the α-factor calculations, has resulted in a molecular understanding of the likely crystal habit surface interaction with the

surrounding solution, along with the solvent effect on the interfacial roughening of the individual crystal surfaces. Both can have a significant effect on the face-specific crystal growth rates and therefore should be taken into account when selecting a crystallisation solvent, if it is important to control the crystal morphology. These calculations can provide a valuable guide to optimising the crystallisation conditions that will produce a desirable crystal morphology, which can be important when processing active ingredient crystals into marketable products in the pharmaceutical and fine chemical industries.

Acknowledgement

This work forms part of the PhD studies of one of us (TTHN), for which we gratefully acknowledge the financial support from Pfizer and UK Northern Universities (N8) METRC initiative in molecular engineering.

We also gratefully acknowledge the UK's EPSRC for their support in nucleation research at the Universities of Leeds and Manchester through their funding of the Critical Mass Project "Molecules, Clusters and Crystals" (grant references EP/I014446/1 and EP/I013563/1, respectively).

We also gratefully acknowledge the funding provided from the 'Advanced Digital Design of Pharmaceutical Therapeutics' (ADDOPT) project, funded by the UK's Advanced Manufacturing Supply Chain Initiative (AMSCI).

Finally, we wish to gratefully acknowledge helpful comments from Professor Robert Sekerka (Carnegie Mellon University, USA), Professor Helmut Klapper (Technical University of Aachen)

and Dr Diana Camacho Corzo (University of Leeds, UK) concerning the analysis of the re-entrant features and crystallographic zone analysis.

References

1. Bunyan, J.; Shankland, N.; Sheen, D. In *Solvent effects on the morphology of ibuprofen*, AIChE Symposium Series1991; pp 44-54.

2. Nguyen, T. T. H.; Hammond, R. B.; Roberts, K. J.; Marziano, I.; Nichols, G., Precision measurement of the growth rate and mechanism of ibuprofen {001} and {011} as a function of crystallization environment. *CrystEngComm* **2014,** *16*, 4568-4586.

3. Hammond, R. B.; Hashim, R. S.; Ma, C.; Roberts, K. J., Grid-based molecular modeling for pharmaceutical salt screening: Case example of 3, 4, 6, 7, 8, 9-hexahydro-2H-pyrimido (1, 2-a) pyrimidinium acetate. *Journal of Pharmaceutical Sciences* **2006,** *95*, 2361-2372.

4. Hammond, R. B.; Ma, C.; Roberts, K. J.; Ghi, P. Y.; Harris, R. K., Application of systematic search methods to studies of the structures of urea-dihydroxy benzene cocrystals. *The Journal of Physical Chemistry B* **2003,** *107*, 11820-11826.

5. Hartman, P.; Bennema, P., The attachment energy as a habit controlling factor: I. Theoretical considerations. *Journal of Crystal Growth* **1980,** *49*, 145-156.

6. Roberts, K.; Docherty, R.; Bennema, P.; Jetten, L., The importance of considering growth-induced conformational change in predicting the morphology of benzophenone. *Journal of Physics D: Applied Physics* **1993,** *26*, B7.

7. Sun, C. C., Materials science tetrahedron—A useful tool for pharmaceutical research and development. *Journal of Pharmaceutical Sciences* **2009,** *98*, 1671-1687.

8. Walker, E. M.; Roberts, K. J.; Maginn, S. J., A molecular dynamics study of solvent and impurity interaction on the crystal habit surfaces of epsilon-caprolactam. *Langmuir* **1998,** *14*, 5620-5630.

9. Winn, D.; Doherty, M. F., Modeling crystal shapes of organic materials grown from solution. *AIChE journal* **2000,** *46*, 1348-1367.

10. Hammond, R. B.; Hashim, R. S.; Ma, C.; Roberts, K. J., Grid-based molecular modeling for pharmaceutical salt screening: Case example of 3,4,6,7,8,9-hexahydro-2H-pyrimido (1,2-a) pyrimidinium acetate. *Journal of Pharmaceutical Sciences* **2006,** *95*, 2361-2372.

11. Hammond, R. B.; Pencheva, K.; Roberts, K. J., A Structural−Kinetic Approach to Model Face-Specific Solution/Crystal Surface Energy Associated with the Crystallization of Acetyl Salicylic Acid from Supersaturated Aqueous/Ethanol Solution. *Cryst Grow Des* **2006,** *6*, 1324-1334.

12. Hammond, R. B.; Pencheva, K.; Ramachandran, V.; Roberts, K. J., Application of grid-based molecular methods for modeling solvent-dependent crystal growth morphology: Aspirin crystallized from aqueous ethanolic solution. *Cryst Grow Des* **2007,** *7*, 1571-1574.

13. Hammond, R. B.; Pencheva, K.; Roberts, K. J., Molecular modeling of crystal-crystal interactions between the alpha- and beta-polymorphic forms of L-glutamic acid using grid-based methods. *Crystal Growth & Design* **2007,** *7*, 875-884.

14. Price, S. L., Computational prediction of organic crystal structures and polymorphism. *International Reviews in Physical Chemistry* **2008,** *27*, 541-568.

15. Hammond, R. B.; Jeck, S.; Ma, C. Y.; Pencheva, K.; Roberts, K. J.; Auffret, T., An Examination of Binding Motifs Associated With Inter-Particle Interactions between Facetted Nano-Crystals of Acetylsalicylic Acid and Ascorbic Acid through the Application of Molecular Grid-Based Search Methods. *Journal of Pharmaceutical Sciences* **2009,** *98*, 4589-4602.

16. Hammond, R. B.; Ramachandran, V.; Roberts, K. J., Molecular modelling of the incorporation of habit modifying additives: [small alpha]-glycine in the presence of l-alanine. *CrystEngComm* **2011,** *13*, 4935-4944.

17. Ramachandran, V.; Murnane, D.; Hammond, R. B.; Pickering, J.; Roberts, K. J.; Soufian, M.; Forbes, B.; Jaffari, S.; Martin, G. P.; Collins, E.; Pencheva, K., Formulation Pre-screening of Inhalation Powders Using Computational Atom–Atom Systematic Search Method. *Molecular Pharmaceutics* **2014,** *12*, 18-33.

18. Rosbottom, I. The Influence of Molecular Interactions and Aggregation on the Polymorphism, Crystal Growth and Morphology of Para Amino Benzoic Acid University of Leeds, Leeds, 2015.

19. Pallipurath, A. R.; Civati, F.; Eziashi, M.; Omar, E.; McArdle, P.; Erxleben, A., Tailoring Cocrystal and Salt Formation and Controlling the Crystal Habit of Diflunisal. *Crystal Growth & Design* **2016,** *16*, 6468-6478.

20. McArdle, P., Oscail, a program package for small-molecule single-crystal crystallography with crystal morphology prediction and molecular modelling. *Journal of Applied Crystallography* **2017,** *50*, 320-326.

21. Dunitz, J. D.; Gavezzotti, A., Molecular Recognition in Organic Crystals: Directed Intermolecular Bonds or Nonlocalized Bonding? *Angewandte Chemie International Edition* **2005,** *44*, 1766-1787.

22. Desiraju, G.; Vittal, J. J.; Ramanan, A., *Crystal Engineering: The Design of Organic Solids*. Elsevier1989.

23. Desiraju, G. R., Supramolecular Synthons in Crystal Engineering—A New Organic Synthesis. *Angewandte Chemie International Edition in English* **1995,** *34*, 2311-2327.

24. (Editor) Roberts, K. J.; (Editor) Docherty, R.; (Editor) Tamura, R., *Engineering Crystallography: From Molecule to Crystal to Functional Form*. 2017 (In Press).

25. Roberts, K. J.; Hammond, R. B.; Ramachandran, V.; Docherty, R., Synthonic engineering: from molecular and crystallographic structure to the rational design of pharmaceutical solid dosage forms. In *Computational Approaches in Pharmaceutical Solid State Chemistry* Abramov, Y., Ed. Wiley: New Jersey, USA, 2016.

26. Bravais, A., *Etudes Crystallographiques*. Gauthiers Villars: Paris, 1886.

27. Friedel, G., *Bulletin De La Societe Francaise De Mineralogie Et De Crystallographie* **1907,** *30*, 326.

28. Donnay, J. D. H.; Harker, D., A new law of crystal morphology extending the law of bravais. *Am Mineral* **1937,** *22*, 446-467.

29. Hartman, P.; Perdok, W. G., On the relations between structure and morphology of crystals. I. *Acta Crystallogr* **1955,** *8*, 49-52.

30. Hartman, P.; Bennema, P., The attachment energy as a habit controlling factor: I. Theoretical considerations. *J Cryst Growth* **1980,** *49*, 145-156.

31. Docherty, R.; Roberts, K. J., Modeling The Morphology Of Molecular-Crystals - Application To Anthracene, Biphenyl And Beta-Succinic Acid. *J. Cryst. Growth* **1988,** *88*, 159-168.

32. Docherty, R.; Clydesdale, G.; Roberts, K. J.; Bennema, P., Application Of Bravais-Friedel-Donnay-Harker, Attachment Energy And Ising-Models To Predicting And Understanding The Morphology Of Molecular-Crystals. *J. Phys. D-Appl. Phys.* **1991,** *24*, 89-99.

33. Roberts, K. J.; Docherty, R.; Bennema, P.; Jetten, L., The Importance Of Considering Growth-Induced Conformational Change In Predicting The Morphology Of Benzophenone. *J. Phys. D-Appl. Phys.* **1993,** *26*, B7-B21.

34. Rosbottom, I.; Roberts, K. J.; Docherty, R., The solid state, surface and morphological properties of p-aminobenzoic acid in terms of the strength and directionality of its intermolecular synthons. *CrystEngComm* **2015,** *17*, 5768-5788.

35. Burton, W. K.; Cabrera, N.; Frank, F. C., The Growth Of Crystals And The Equilibrium Structure Of Their Surfaces. *Philos T Roy Soc A* **1951,** *243*, 299-358.

36. Ohara, M.; Reid, R. C., *Modelling Crystal Growth Rates*. 1974.

37. Winn, D.; Doherty, M. F., A new technique for predicting the shape of solution-grown organic crystals. *Aiche Journal* **1998,** *44*, 2501-2514.

38. Lovette, M. A.; Doherty, M. F., Needle-Shaped Crystals: Causality and Solvent Selection Guidance Based on Periodic Bond Chains. *Cryst Grow Des* **2013,** *13*, 3341-3352.

39. Chen, J.; Trout, B. L., Computer-Aided Solvent Selection for Improving the Morphology of Needle-like Crystals: A Case Study of 2,6-Dihydroxybenzoic Acid. *Crystal Grow Des* **2010,** *10*, 4379-4388.

40. Tilbury, C. J.; Green, D. A.; Marshall, W. J.; Doherty, M. F., Predicting the Effect of Solvent on the Crystal Habit of Small Organic Molecules. *Crystal Growth & Design* **2016,** *16*, 2590-2604.

41. Li, J.; Tilbury, C. J.; Joswiak, M. N.; Peters, B.; Doherty, M. F., Rate Expressions for Kink Attachment and Detachment During Crystal Growth. *Crystal Growth & Design* **2016,** *16*, 3313-3322.

42. Bourne, J. R.; Davey, R. J., The role of solvent-solute interactions in determining crystal growth mechanisms from solution. *J. Cryst. Growth* **1976,** *36*, 278-286.

43. Bourne, J. R.; Davey, R. J., The role of solvent-solute interactions in determining crystal growth mechanisms from solution: II. The growth kinetics of hexamethylene tetramine. *J. Cryst. Growth* **1976,** *36*, 287-296.

44. Toroz, D.; Rosbottom, I.; Turner, T. D.; Corzo, D. M. C.; Hammond, R. B.; Lai, X.; Roberts, K. J., Towards an understanding of the nucleation of alpha-para amino benzoic acid from ethanolic solutions: a multi-scale approach. *Faraday Discussions* **2015,** *179*, 79-114.

45. Jackson, K. A., *Mechanism of Growth in Liquid Metals and Solidification*. Cleveland, 1958.

46. Bennema, P., Morphology of crystals determined by alpha factors, roughening temperature, F faces and connected nets. *Journal of Physics D: Applied Physics* **1993,** *26*, B1.

47. Bennema, P.; van der Eerden, J. P., Crystal growth from solution: Development in computer simulation. *Journal of Crystal Growth* **1977,** *42*, 201-213.

48. Human, H. J.; Van Der Eerden, J. P.; Jetten, L. A. M. J.; Odekerken, J. G. M., On the roughening transition of biphenyl: Transition of faceted to non-faceted growth of biphenyl for growth from different organic solvents and the melt. *J. Cryst. Growth* **1981,** *51*, 589-600.

49. Davey, R., The Role of Additives in Precipitation Processes, Industrial Crystallization 81, SJ Jancic and EJ de Jong, Eds. North-Holland Publishing Co1982.

50. Jetten, L. A. M. J.; Human, H. J.; Bennema, P.; Van Der Eerden, J. P., On the observation of the roughening transition of organic crystals, growing from solution. *Journal of Crystal Growth* **1984,** *68*, 503-516.

51. Davey, R., The role of the solvent in crystal growth from solution. *Journal of Crystal Growth* **1986,** *76*, 637-644.

52. McConnell, J. F., 2-(4-Isobuthylphenyl) propionic acid. $C_{13}H_{18}O_2$ ibuprofen or prufen. *Cryst. Struct. Commun.* **1974,** *3*, 73-75.

53. Mayo, S. L.; Olafson, B. D.; Goddard, W. A., Dreiding - A Generic Force-Field For Molecular Simulations. *J Phys Chem* **1990,** *94*, 8897-8909.

54. Stewart, J., MOPAC 6.0,(CQCPE program# 455). Quantum Chemistry Program Exchange, Creative Arts Building 181, Indiana University, Bloomington, IN 47405 USA.

55. Dewar, M. J. S.; Zoebisch, E. G.; Healy, E. F.; Stewart, J. J. P., Development and use of quantum mechanical molecular models. 76. AM1: a new general purpose quantum mechanical molecular model. *Journal of the American Chemical Society* **1985,** *107*, 3902-3909.

56. Clydesdale, G.; Roberts, K. J.; Docherty, R., Modelling the morphology of molecular crystals in the presence of disruptive tailor-made additives. *J. Cryst. Growth* **1994,** *135*, 331-340.

57. Clydesdale, G.; Roberts, K. J.; Telfer, G. B.; Grant, D. J. W., Modeling the crystal morphology of α-lactose monohydrate. *Journal of Pharmaceutical Sciences* **1997,** *86*, 135-141.

58. Hammond, R. B.; Roberts, K. J.; Smith, E. D. L.; Docherty, R., Application of a Computational Systematic Search Strategy to Study Polymorphism in Phenazine and Perylene. *The Journal of Physical Chemistry B* **1999,** *103*, 7762-7770.

59. Hammond, R. B.; Ma, C.; Roberts, K. J.; Ghi, P. Y.; Harris, R. K., Application of Systematic Search Methods to Studies of the Structures of Urea−Dihydroxy Benzene Cocrystals. *The Journal of Physical Chemistry B* **2003,** *107*, 11820-11826.

60. Hammond, R. B.; Pencheva, K.; Roberts, K. J., Simulation of energetic stability of facetted L-glutamic acid nanocrystalline clusters in relation to their polymorphic phase stability as a function of crystal size. *Journal of Physical Chemistry B* **2005,** *109*, 19550-19552.

61. Grančič, P.; Bylsma, R.; Meekes, H.; Cuppen, H. M., Evaluation of All-Atom Force Fields for Anthracene Crystal Growth. *Crystal Growth & Design* **2015,** *15*, 1625-1633.

62. Inc, A. S. *Materials Studio* 5.5: San Diego, 2011.

63. Clydesdale, G.; Docherty, R.; Roberts, K., HABIT-a program for predicting the morphology of molecular crystals. *Computer Physics Communications* **1991,** *64*, 311-328.

64. Docherty, R.; Roberts, K. J.; Dowty, E., Morang — A computer program designed to aid in the determinations of crystal morphology. *Comput Phys Commun* **1988,** *51*, 423-430.

65. Dowty, E., Computing and drawing crystal shapes. *Am. mineral* **1980,** *65*, 465-472.

66. Bennema, P.; Gilmer, G.; Hartman, P., Crystal Growth: An Introduction. *North-Holland, Amsterdam* **1973**, 263.

67. McArdle, P.; Hu, Y.; Lyons, A.; Dark, R., Predicting and understanding crystal morphology: the morphology of benzoic acid and the polymorphs of sulfathiazole. *CrystEngComm* **2010,** *12*, 3119-3125.

68. Walshe, N.; Crushell, M.; Karpinska, J.; Erxleben, A.; McArdle, P., Anisotropic Crystal Growth in Flat and Nonflat Systems: The Important Influence of van der Waals Contact Molecular Stacking on Crystal Growth and Dissolution. *Crystal Grow Des* **2015,** *15*, 3235-3248.

69. Lukman, Z.; Anuar, N.; Abdul Rahman, N., Racemic Ibuprofen Morphology: Molecular Modelling and Experimental. *Advanced Materials Research* **2015,** *1113*, 504-510.

70. Cano, H.; Gabas, N.; Canselier, J., Experimental study on the ibuprofen crystal growth morphology in solution. *Journal of Crystal Growth* **2001,** *224*, 335-341.

71. Rashid, M. A., Crystallization engineering of ibuprofen for pharmaceutical formulation. **2011**.

72. Griesser, U.; Hilfiker, R., Polymorphism in the Pharmaceutical Industry. *ed. Rolf Hilfiker, Wiley-VCH Verlag GmbH & Co* **2006**, 211-233.

73. Camacho, D. M.; Roberts, K. J.; Lewtas, K.; More, I., The crystal morphology and growth rates of triclinic N-docosane crystallising from N-dodecane solutions. *Journal of Crystal Growth* **2015,** *416*, 47-56.

74. Sekerka, R. F., Role of instabilities in determination of the shapes of growing crystals. *Journal of Crystal Growth* **1993,** *128*, 1-12.

75. Serkerka, R., 2014.

For Table of Contents Use Only

Crystal morphology and interfacial stability of RS-Ibuprofen in relation to its molecular and synthonic structure

T. T. H. Nguyen[+], I. Rosbottom, R. B. Hammond, K. J. Roberts*

A combination of the molecular modelling of synthonic strength and the α-factor calculations has aided in a molecular understanding crystal/solution interactions of RS-ibuprofen and their effect on crystal morphology, along with the solvent effect on the interfacial roughening of the individual crystal surfaces. This technique provides a valuable guide for optimising crystallisation conditions that will produce a desirable crystal morphology.